



Enhanced tetragonality and large negative thermal expansion in a new Pb/Bi-based perovskite ferroelectric of $(1-x)\text{PbTiO}_3\text{-xBi}(\text{Zn}_{1/2}\text{V}_{1/2})\text{O}_3$

Journal:	<i>Inorganic Chemistry Frontiers</i>
Manuscript ID	QI-RES-04-2019-000450.R1
Article Type:	Research Article
Date Submitted by the Author:	20-May-2019
Complete List of Authors:	<p>Pan, Zhao; Tokyo Institute of Technology - Suzukakedai Campus, Chen, Jun; University of Science and Technology Beijing, Department of Physical Chemistry Jiang, Xingxing; Beijing Center for Crystal R&D, Key Lab of Functional Crystals and Laser Technology of Chinese Academy of Sciences, Technical Institute of Physics and Chemistry, Chinese Academy of Sciences, ; University of Chinese Academy of Sciences, Lin, Zheshuai; Technical Institute of Physics and Chemistry, Chinese Academy of Sciences, Zhang, Haibo; Huazhong University of Science and Technology - Main Campus Ren, Yang; Argonne National Laboratory, X-ray Science Division Azuma, Masaki; Tokyo Institute of Technology, Materials and Structures Laboratory Xing, Xianran; University of Science and Technology Beijing, School of Metallurgical and Ecological Engineering</p>



Journal Name

ARTICLE

Enhanced tetragonality and large negative thermal expansion in a new Pb/Bi-based perovskite ferroelectric of $(1-x)\text{PbTiO}_3$ - $x\text{Bi}(\text{Zn}_{1/2}\text{V}_{1/2})\text{O}_3$

Received 00th January 20xx,
Accepted 00th January 20xx

DOI: 10.1039/x0xx00000x

Zhao Pan,^{a,b,*} Jun Chen,^c Xingxing Jiang,^d Zheshuai Lin,^d Haibo Zhang,^a Yang Ren,^e Masaki Azuma^{b,*} and Xianran Xing^c

The exploring of large Negative thermal expansion (NTE) over a wide temperature range is an important subject in materials science, since the overall coefficient of thermal expansion (CTE) of ordinary materials can be effectively tailored by the introduction of NTE materials. Here we successfully achieved a large NTE within broad temperature range in a new Pb/Bi-based ferroelectric of $(1-x)\text{PbTiO}_3$ - $x\text{Bi}(\text{Zn}_{1/2}\text{V}_{1/2})\text{O}_3$ by means of improving the ferroelectricity of PbTiO_3 . The present system exhibits an unusual enhanced tetragonality, large spontaneous polarization (P_s), and high Curie temperature (T_C). Specifically, the $x = 0.1$ compound exhibits an enhanced CTE of $-2.10 \times 10^{-5}/^\circ\text{C}$ from room temperature (RT) up to its T_C of 600°C , which is contrasted to that of pristine PbTiO_3 ($-1.99 \times 10^{-5}/^\circ\text{C}$, RT - 490°C). More intriguingly, a large volume shrinkage ($\Delta V \approx -1\%$) has also been observed during the ferroelectric-to-paraelectric phase transition. According to the experimental and theoretical studies, the large NTE is attributed to the enhanced P_s derived from the strong hybridization of Pb/Bi-O and Ti/Zn/V-O through the substitution of polar $\text{Bi}(\text{Zn}_{1/2}\text{V}_{1/2})\text{O}_3$ perovskite. The present study demonstrates that large NTE within wide temperature range can be achieved in PbTiO_3 -based ferroelectrics by improving its ferroelectricity through introducing isostructural polar perovskites.

Introduction

Most materials display positive thermal expansion (PTE) upon heating. However, although rare, several categories of materials exhibit negative thermal expansion (NTE), in which the volume unusually contracts on heating. There are a number of important potential applications for materials with a negative coefficient of thermal expansion (CTE). Perhaps the most immediate one is in composite materials where the overall CTE can be precisely tailored to be a specific positive, negative or even zero value.¹⁻⁶ The origin of NTE materials have been well studied in the past decades, mainly including the phonon-related transverse cooperative vibration (e.g., ZrW_2O_8 , $\text{Ag}_3[\text{Co}(\text{CN})_6]$, and ScF_3),⁷⁻¹⁰ the magnetovolume effect (e.g., Invar alloys and Mn_3AN),¹¹⁻¹⁴ the intermetallic charge transfer (e.g., $\text{LaCu}_3\text{Fe}_4\text{O}_{12}$ and BiNiO_3),^{15,16} the metal-insulator transition (e.g.,

CuRuO_3),^{17,18} and the spontaneous volume ferroelectrostriction (SVFS) in PbTiO_3 -based ferroelectrics.^{19,20} Recent studies in the field of NTE materials have focused on large NTE over a wide temperature range, due to the fact that normally the stronger the NTE is, the more efficient it is to counteract PTE within composite materials.^{2,4}

Among the available NTE materials, there is one branch of ferroelectrics which exhibit a general phenomenon that the unit cell volume shrinkages during the ferroelectric-to-paraelectric (FE-PE) phase transition, such as perovskites of PbTiO_3 ,²¹⁻²³ BaTiO_3 ,²⁴ (Bi, La) NiO_3 ,¹⁶ and recently reported $\text{CH}_3\text{NH}_3\text{PbI}_3$,²⁵ tungsten bronze of PbNb_2O_6 ,²⁶ and tin-hypothiodiphosphate of $\text{Sn}_2\text{P}_2\text{S}_6$.²⁷ However, all the ferroelectrics except PbTiO_3 , in which the NTE behavior occurs from room temperature to its Curie temperature (T_C) of 490°C , exhibit NTE property in a relative narrow temperature range.²⁸ Such a wide NTE range of PbTiO_3 provides the opportunity to modify the NTE property, i.e., achieving large NTE over a wide temperature range. The origin of NTE in PbTiO_3 -based ferroelectrics has recently been well studied by the SVFS effect, which determines the crucial role of ferroelectric behavior on the NTE.¹⁹ Below T_C , PbTiO_3 exhibits ferroelectricity and NTE, while NTE disappears in the paraelectric phase above T_C . In the ferroelectric phase, the increased volume can be well maintained by the large tetragonality (c/a) resulted from the strong spontaneous polarization (P_s). It is noteworthy that NTE in PbTiO_3 -based ferroelectrics is mainly attributed to shrinkage of the polar c axis. Based on these, it is

^a School of Materials Science and Engineering, Huazhong University of Science and Technology, Wuhan 430074, China. E-mail: zhaopan@mssl.titech.ac.jp

^b Laboratory for Materials and Structures, Tokyo Institute of Technology, 4259 Nagatsuta, Midori, Yokohama, 226-8503, Japan. E-mail: mazuma@mssl.titech.ac.jp

^c Department of Physical Chemistry, University of Science and Technology Beijing, Beijing 100083, China.

^d Institute of Physics and Chemistry, Chinese Academy of Sciences, Beijing 100190, China

^e X-Ray Science Division, Argonne National Laboratory, Argonne, Illinois 60439, United States.

† Footnotes relating to the title and/or authors should appear here.

Electronic Supplementary Information (ESI) available: [details of any supplementary information available should be included here]. See DOI: 10.1039/x0xx00000x

therefore proposed that large NTE could be obtained through improving the c/a of PbTiO_3 .

$\text{Bi}(\text{Zn}_{1/2}\text{V}_{1/2})\text{O}_3$ is recently reported to be a new PbTiO_3 -type perovskite, which exhibits rather larger tetragonality ($c/a = 1.26$) and stronger polarization ($P_s = 126 \mu\text{C}/\text{cm}^2$) compared to those of PbTiO_3 ($c/a = 1.064$, $P_s = 59 \mu\text{C}/\text{cm}^2$).^{29,30} The introduction of $\text{Bi}(\text{Zn}_{1/2}\text{V}_{1/2})\text{O}_3$ in PbTiO_3 is considered to further increase its tetragonality, and therefore achieving enhanced NTE. Herein, we successfully achieved large NTE over a wide temperature range in the present new Pb/Bi-based binary system of $(1-x)\text{PbTiO}_3$ - $x\text{Bi}(\text{Zn}_{1/2}\text{V}_{1/2})\text{O}_3$. A continuously enhanced c/a has been observed by the substitution of polar $\text{Bi}(\text{Zn}_{1/2}\text{V}_{1/2})\text{O}_3$ perovskite. As expected, both the NTE and T_c have been improved to a certain extent. In particular, remarkably volume shrinkages have also been observed in $(1-x)\text{PbTiO}_3$ - $x\text{Bi}(\text{Zn}_{1/2}\text{V}_{1/2})\text{O}_3$ during the FE-PE phase transition, which have been well studied by the experimental and theoretical results.

Experimental section

Materials synthesis and measurements

Polycrystalline samples of $(1-x)\text{PbTiO}_3$ - $x\text{Bi}(\text{Zn}_{1/2}\text{V}_{1/2})\text{O}_3$ (hereafter abbreviated as $(1-x)\text{PT-xBZV}$, $x = 0.1 - 0.5$) were prepared by a cubic anvil-type high-pressure apparatus. The raw materials of PbO , Bi_2O_3 , ZnO , TiO_2 , V_2O_3 , and V_2O_5 were stoichiometrically mixed and sealed in a gold capsule, and then treated at 6 GPa and 1100 °C for 30 min. After the high-pressure process, the obtained compounds were carefully ground in an agate mortar, and subsequently annealed at 400 °C for 4 hours. The X-ray diffraction (XRD) patterns were collected with a Bruker D8 ADVANCE diffractometer for phase identification. The high-temperature synchrotron powder diffraction (SXRD) experiment was conducted at the 11-ID-C beamline of the Advanced Photon Source with the light wavelength of 0.117418 Å.

Computational

First-principles calculation was performed by using CASTEP,³¹ a total energy package based on plane-wave pseudopotential density functional theory (DFT).^{32,33} The correlation and exchange energy was described by Perdew, Burke and Ernzerhof (PBE)³⁴ in generalized gradient approximation (GGA)³⁵ form. The optimized norm-conserving pseudopotential³⁶ in Kleinman-Bylander³⁷ form were adopted to model the effective interaction between the valence electrons and atom cores, allowing the choice of a relatively small plane-wave basis set without compromising the computational accuracy. The disorder occupation in 0.5PbTiO_3 - $0.5\text{Bi}(\text{Zn}_{1/2}\text{V}_{1/2})\text{O}_3$ was handled by virtual crystal approximation (VCA),³⁸ in which the disorder position is modeled a ghost atom with the effective Coulomb potential weighted by its atomic constitution. Kinetic energy cutoff 800 eV and Monkhorst-Pack³⁹ with k-point meshes less than 0.03 \AA^{-1} in the Brillouin zones were chosen.

Results and Discussion

The laboratory XRD patterns of $(1-x)\text{PT-xBZV}$ from $x = 0.1$ to 0.5 are shown in Figure 1(a). As can be seen, all the investigated compounds exhibit a single tetragonal phase without any noticeable impurities. With the substitution of BZV, the (001) peak shows a clear shift to the lower angle, indicating the expansion of c axis. While the (100) peak exhibits an opposite trend, it shifts slightly to the higher angle which demonstrates the shrinkage of $a(b)$ axis. The detailed lattice parameters were refined and plotted in Figure 1(b). The c axis increases almost linearly, whereas $a(b)$ axis decrease continuously as a function of BZV. Consequently, an

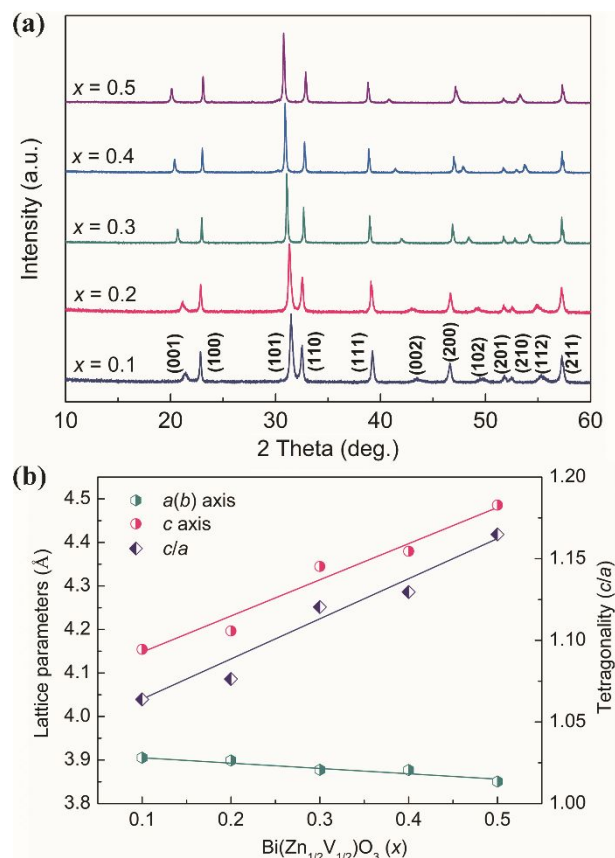


Figure 1. (a) XRD patterns and (b) lattice parameters of $(1-x)\text{PT-xBZV}$ ($x = 0.1 - 0.5$) at room temperature.

unusually enhanced c/a has been observed. The c/a value increases from 1.06 of pristine PT to 1.08, 1.12, 1.13, and 1.16 of $x = 0.1, 0.2, 0.3, 0.4,$ and 0.5 , respectively, which suggests the substitution of BZV effectively enhanced the tetragonality of PT. Here the large tetragonality results in a pyramidal rather than an octahedral coordination in the $(1-x)\text{PT-xBZV}$ solid solutions (see top left of Figure 2). The large lattice distortion can be attributed to the large P_s displacements induced by the strong Pb/Bi-O hybridization and coupling interactions between Ti/Zn/V and Pb/Bi cations, which can be evidenced by the following theoretical calculations.

It is well known that in ABO_3 perovskite-type ferroelectrics P_s originates from the displacements from the centroid of the oxygen polyhedrons of the A site and B site atoms (see bottom right of Figure 2).²¹ Here the P_s displacements of A site Pb/Bi and B site

Ti/Zn/V cations can be derived from the SXRD refinement results. The detailed structure of (1-x)PT-xBZV were refined using the Rietveld method with the *FullProf* software. The initial structural model corresponds to PbTiO₃ with the atomic positions being given in the noncentrosymmetric space group *P4mm* (No. 99).⁴⁰ The occupancies of atoms were fixed at the ideal composition. The isotropic thermal factors of Pb/Bi, Zn/Ti/V, as well as O(I) and O(II) were set equal, respectively. In addition, the anisotropic profile broadening model has been adopted in order to obtain good fitting results.⁴¹ As can be seen, the calculated diffraction profiles agree well with the observed ones (Figure S1 to S5). The related P_s can be estimated by considering a purely ionic crystal and neglecting the electronic polarization by using the following formula,⁴²

$$P_s = Z \sum_i \frac{\delta z_i q_i}{V}$$

Where δz_i indicates the cation shifts along with the ferroelectric axis of the *i*th ion with the electric charge q_i , V represents the unit cell volume, and Z equals to 1. As shown in Figure 2, the calculated P_s increases continuously with the solubility of BZV, ranging from 66, 70, 83, 93, to as large as 97 $\mu\text{C}/\text{cm}^2$ for $x = 0.1, 0.2, 0.3, 0.4,$ and 0.5 , respectively, which are much larger than that of pristine PbTiO₃ (59 $\mu\text{C}/\text{cm}^2$).³⁰ The refined results indicate that the substitution of BZV enhanced the P_s , which is consistent with the enhanced tetragonality.

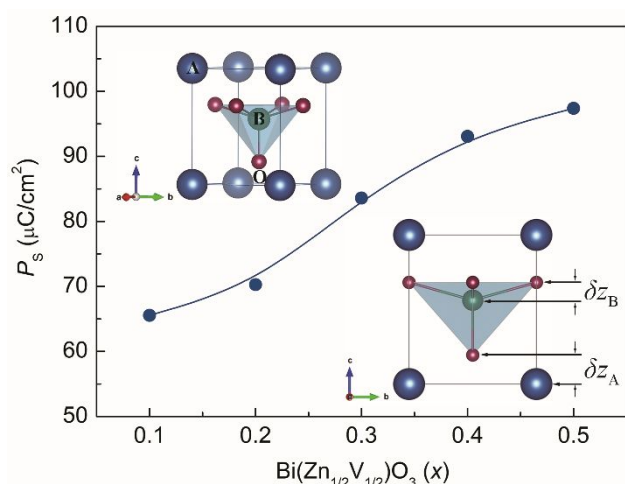


Figure 2. The calculated spontaneous polarization of (1-x)PT-xBZV ($x = 0.1 - 0.5$) at room temperature. The insets are the crystal structure (top left) and schematic diagram of P_s (bottom right).

Both the theoretical and experimental studies have approved that enhanced tetragonality in PbTiO₃-based ferroelectric could give rise to enhanced NTE.^{19,43} Generally, a large c/a indicates large lattice distortion, and could result in large volume shrinkage with high lattice energy releasing during the heating process. As a result, enhanced NTE could be observed, such as in Pb_{1-x}Cd_xTiO₃,⁴⁴ PbTiO₃-BiFeO₃,⁴⁵ and recently reported Pb(Ti_{1-x}V_x)O₃ and (1-x)PbTiO₃-xBiCoO₃ systems,^{20,46} which exhibit abnormal enhanced c/a and NTE compared to those of PbTiO₃. In order to precisely investigate the thermal expansion property of the (1-x)PT-xBZV system, the temperature dependence of SXRD experiments have been conducted (Figure S6 and S7). The detailed unit cell volumes were

extracted by means of structure refinement based on the SXRD data (Figure 3a). With the substitution of BZV, the 0.9PT-0.1BZV

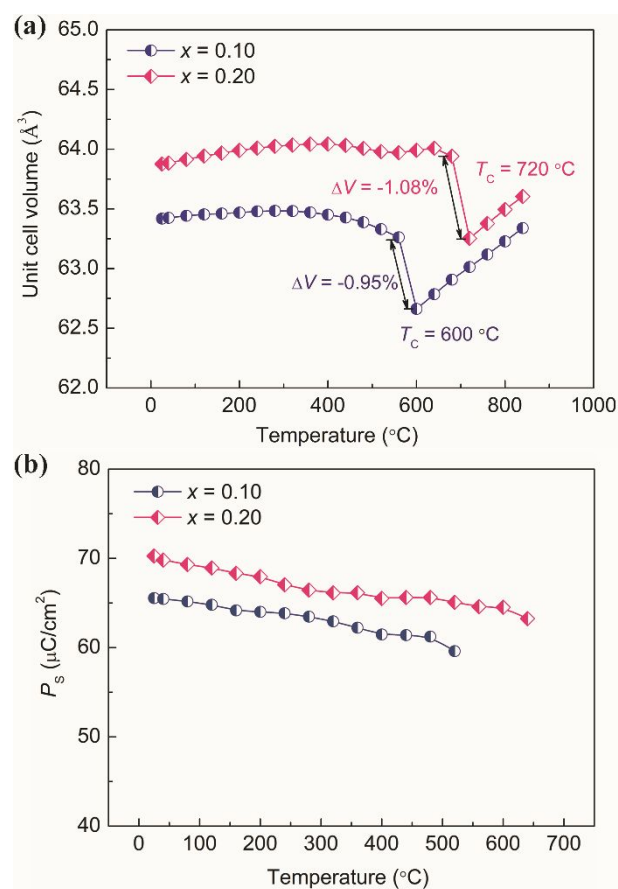


Figure 3. (a) Unit cell volume and (b) the calculated spontaneous polarization of (1-x)PT-xBZV ($x = 0.1$ and 0.2) as a function of temperature.

compound presents a nonlinear and strong NTE in a wide temperature range from room temperature (RT) to near T_c . This is contrasted to pristine BZV, which decomposes at temperature higher than 730 K before reaching its T_c .²⁹ Note that the unit cell volume of 0.9PT-0.1BZV shows little dependence on temperature before the FE-PE phase transition. However, it contracts dramatically during the FE-PE phase transition. A noticeable volume shrinkage of -0.95% has been observed during the phase transition. The average CTE of the overall temperature range is $-2.10 \times 10^{-5}/^\circ\text{C}$ (RT ~ 600 °C). With further increasing the content of BZV, the compound of 0.8PT-0.2BZV shows a tendency of PTE with a negligible CTE of $1.56 \times 10^{-6}/^\circ\text{C}$ (RT ~ 680 °C) before the FE-PE phase transition. Intriguingly, a more pronounced volume contraction as large as -1.08% has been observed during the FE-PE phase transition. In comparison, the present NTE is among the giant NTE materials such as CuO nanoparticles (-1.1%),⁴⁷ Mn₃AN (-1.3%),¹² BiNiO₃ (-2.5%),¹⁶ Ca₂RuO_{3.74} (-1.0%),¹⁸ and recently reported Pb_{0.76}La_{0.04}Bi_{0.20}VO₃ (-6.7%).⁴⁸ It is worth noting that the present compound of 0.9PT-0.1BZV ($-2.10 \times 10^{-5}/^\circ\text{C}$, RT ~ 600 °C) not only enhances the NTE of PT ($-1.99 \times 10^{-5}/^\circ\text{C}$, RT ~ 490 °C) but also extends the NTE to a much wider temperature range. The T_c of PT has been significantly increased by 100 °C, which is attributed to the enhanced polarization according to the empirical relationship of $T_c = \alpha P_s^2$.³⁰ For further increasing the content of BZV, the

compounds decompose before reaching the FE-PE phase transition temperature, which is ascribed to the increased lattice distortion and weakened thermal stability of the perovskite structure.

$0.5\text{PbTiO}_3\text{-}0.5\text{BiZn}_{0.5}\text{V}_{0.5}\text{O}_3$, the electron-concentration strongly dominates in the chemical bonds within the pyramidal anions. Moreover, the highest value of the electronic density difference in PbTiO_3 is 3.75\AA^{-3} , which is smaller than that in $0.5\text{PbTiO}_3\text{-}$

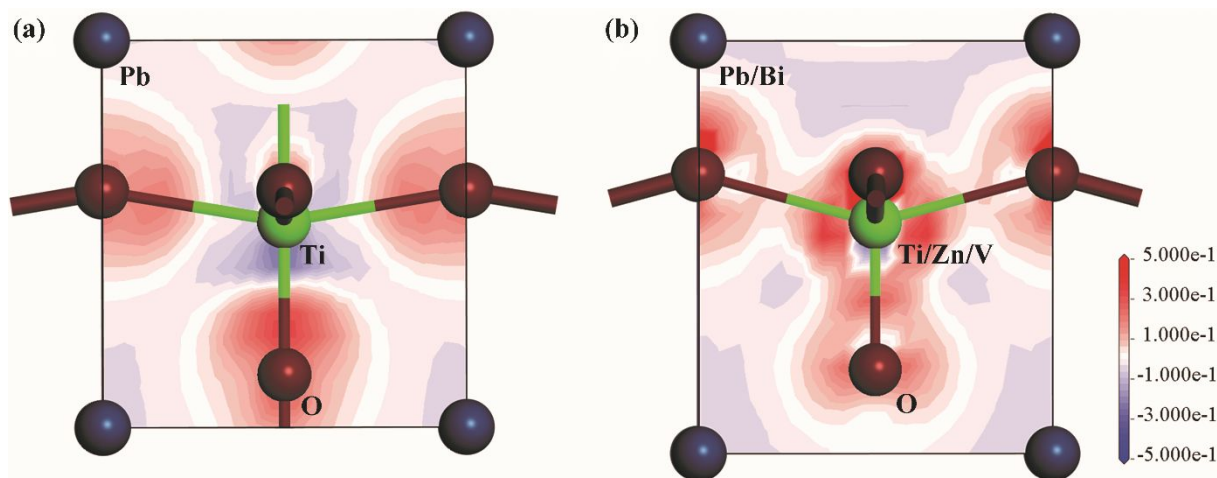


Figure 4. The electronic density difference map of (a) PbTiO_3 and (b) $0.5\text{PbTiO}_3\text{-}0.5\text{BiZn}_{0.5}\text{V}_{0.5}\text{O}_3$. The Pb(Pb/Bi), Ti(Ti/Zn/V), and O atoms are indicated by black blue, green, and violet balls, respectively.

Recently, a new concept of spontaneous volume ferroelectrostriction (SVFS) has been proposed to illuminate the origin of NTE in PbTiO_3 -based ferroelectrics.¹⁹ According to the description of SVFS, the ferroelectric behavior plays an important role in the NTE of PT-based ferroelectrics. The NTE of PT-based ferroelectrics generally occurs in the ferroelectric phase, while it disappears in the paraelectric phase. The increased volume in the ferroelectric phase can be maintained by the high lattice distortion c/a which results from the large P_S . Therefore, how the P_S , which can reflect the magnitude of ferroelectricity, varies with temperature will directly affect the NTE. The variation of P_S as a function of temperature for $0.9\text{PT-}0.1\text{BZV}$ and $0.8\text{PT-}0.2\text{BZV}$ are shown in Figure 3b. P_S values of both the two compounds exhibit a slightly decreasing tendency with increasing temperature, which is ascribed to the weakened ferroelectricity. As the temperature is raised up to near T_C , P_S still keeps in a high level, with the values of 60 and $65\ \mu\text{C}/\text{cm}^2$ for $0.9\text{PT-}0.1\text{BZV}$ and $0.8\text{PT-}0.2\text{BZV}$, respectively. Correspondingly, the unit cell volumes of $0.9\text{PT-}0.1\text{BZV}$ and $0.8\text{PT-}0.2\text{BZV}$ can be retained close to that of room temperature by the high P_S . As a result, both the two compositions exhibit little temperature dependence of unit cell volumes before reaching their T_C s. However, P_S suddenly disappears on approaching the T_C , resulting in the noticeable volume shrinkages during the FE-to-PE phase transition.

To further study the effect of BZV substitution on the hybridization with oxygen atoms, the electron density difference of $(1-x)\text{PT-}x\text{BZV}$ ($x = 0$ and 0.5) was calculated by first-principles calculation. As depicted in Figure 4, it is revealed that in both PbTiO_3 and $0.5\text{PbTiO}_3\text{-}0.5\text{Bi}(\text{Zn}_{0.5}\text{V}_{0.5})\text{O}_3$, the concentration of the valence electrons on the Ti-O (or $\text{Ti}_{0.5}\text{Zn}_{0.25}\text{V}_{0.25}\text{-O}$) bond along c -axis is more prominent than those within in (a,b) plane, which indicates that the orbital hybridization along c -axis is stronger than that along $a(b)$ -axis. In pristine PbTiO_3 , apart from the electronic cloud concentration, some electron-loss area also occurs. While in

$0.5\text{BiZn}_{0.5}\text{V}_{0.5}\text{O}_3$ ($4.75\ \text{\AA}^{-3}$). These observations demonstrate that the $\text{Zn}_{0.5}\text{V}_{0.5}/\text{Ti}$ substitution strongly enhanced the covalent interaction within $\text{Ti}_{0.5}\text{Zn}_{0.25}\text{V}_{0.25}\text{O}_3$ pyramid, giving rise to the larger spontaneous polarization.

Conclusions

In summary, a new Pb/Bi-based ferroelectric based on $(1-x)\text{PT-}x\text{BZV}$ has been designed to exhibit large NTE over a wide temperature range. Both the tetragonality and Curie temperature are considerably increased. The $0.9\text{PT-}0.1\text{BZV}$ compound exhibits a large NTE with the average CTE of $-2.10 \times 10^{-5}/^\circ\text{C}$ in the temperature range from room temperature up to $600\ ^\circ\text{C}$, which is largely enhanced compared to that of PbTiO_3 . In particular, large volume shrinkages have also been observed in $0.9\text{PT-}0.1\text{BZV}$ and $0.8\text{PT-}0.2\text{BZV}$ during the FE-PE phase transition. The large NTE is closely related to the enhanced P_S due to the substitution of BZV, which has been well elaborated by the experimental and theoretical results. The present study demonstrates that large NTE within extended temperature range could be achieved in PbTiO_3 -based ferroelectrics through improving its ferroelectric property.

Acknowledgements

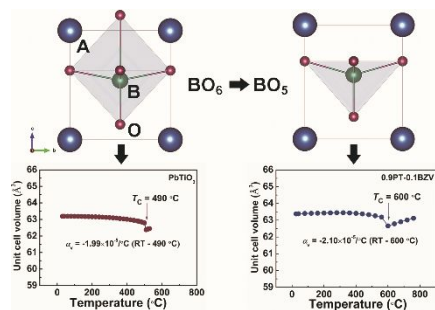
This work was supported by the National Natural Science Foundation of China (Grant Nos. 21805215), National Program for Support of Top-notch Young Professionals, the Program for Changjiang Young Scholars, and the General Financial Grant from the China Postdoctoral Science Foundation (2017M622536). The use of the Advanced Photon Source at Argonne National Laboratory was supported by the U.S.

Department of Energy, Office of Science, Office of Basic Energy Science (DE-AC02-06CH11357).

Notes and references

- 1 J. S. O. Evans, *J. Chem. Soc., Dalton Trans.*, 1999, **19**, 3317-3326.
- 2 K. Takenaka, *Sci. Technol. Adv. Mater.*, 2012, **13**, 013001.
- 3 M. Azuma, K. Oka and K. Nabetani, *Sci. Technol. Adv. Mater.*, 2015, **16**, 034904.
- 4 J. Chen, L. Hu, J. X. Deng and X. R. Xing, *Chem. Soc. Rev.*, 2015, **44**, 3522-3567.
- 5 J. P. Attfield, *Front. Chem.*, 2018, **6**, 371.
- 6 X. Jiang, Y. Yang, M. S. Molocheev, P. F. Gong, F. Liang, S. H. Wang, L. Liu, X. Wu, X. D. Li, Y. C. Li, S. F. Wu, W. Li, Y. C. Wu and Z. S. Lin, *Adv. Mater.*, 2018, **30**, 1801313.
- 7 T. A. Mary, J. S. O. Evans, T. Vogt and A. W. Sleight, *Science*, 1996, **272**, 90-92.
- 8 A. L. Goodwin, M. Calleja, M. J. Conterio, M. T. Dove, J. S. O. Evans, D. A. Keen, L. Peters and M. G. Tucker, *Science*, 2008, **319**, 794-797.
- 9 B. K. Greve, K. L. Martin, P. L. Lee, P. J. Chupas, K. W. Chapman and A. P. Wilkinsom, *J. Am. Chem. Soc.*, 2010, **132**, 15496-15498.
- 10 L. Hu, J. Chen, A. Sanson, H. Wu, C. G. Rodriguez, L. Olivi, Y. Ren, L. L. Fan, J. X. Deng and X. R. Xing, *J. Am. Chem. Soc.*, 2016, **138**, 8320-8323.
- 11 M. Van Schilfgaarde, I. A. Abrikosov and B. Johansson, *Nature*, 1999, **400**, 46-49.
- 12 K. Takenaka and H. Takagi, *Appl. Phys. Lett.*, 2005, **87**, 261902.
- 13 Y. Y. Zhao, F. X. Hu, L. F. Bao, J. Wang, H. Wu, Q. Z. Huang, R. R. Wu, Y. Liu, F. R. Shen, H. Kuang, M. Zhang, W. L. Zuo, X. Q. Zheng, J. R. Sun and B. G. Shen, *J. Am. Chem. Soc.*, 2015, **137**, 1746-1749.
- 14 Y. Sun, C. Wang, Y. C. Wen, L. H. Chu, H. Pan and M. Nie, *J. Am. Ceram. Soc.*, 2010, **93**, 2178-2181.
- 15 Y. W. Long, N. Hayashi, T. Saito, M. Azuma, S. Muranaka and Y. Shimakawa, *Nature*, 2009, **458**, 60-63.
- 16 M. Azuma, W. T. Chen, H. Seki, M. Czapski, S. Olga, K. Oka, M. Mizumaki, T. Watanuki, N. Ishimatsu, N. Kawamura, S. Ishiwata, M. G. Tucker, Y. Shimakawa and J. P. Attfield, *Nat. Commun.*, 2011, **2**, 347.
- 17 T. F. Qi, O. B. Korneta, S. Parkin, L. E. De Long, P. Schlottmann and G. Cao, *Phys. Rev. Lett.*, 2010, **105**, 177203.
- 18 K. Takenaka, Y. Okamoto, T. Shinoda, N. Katayama, Y. Sakai, *Nat. Commun.*, 2017, **8**, 14102.
- 19 J. Chen, F. F. Wang, Q. Z. Huang, L. Hu, X. P. Song, J. X. Deng, R. B. Yu and X. R. Xing, *Sci. Rep.*, 2013, **3**, 2458.
- 20 Z. Pan, J. Chen, X. X. Jiang, L. Hu, R. Z. Yu, H. Yamamoto, T. Ogata, Y. Hattori, F. M. Guo, X. A. Fan, Y. W. Li, G. Q. Li, H. Z. Gu, Y. Ren, Z. S. Lin, M. Azuma and X. R. Xing, *J. Am. Chem. Soc.*, 2017, **139**, 14865-14868.
- 21 J. Chen, X. R. Xing, C. Sun, P. H. Hu, R. B. Yu, X. W. Wang and L. H. Li, *J. Am. Chem. Soc.*, 2008, **130**, 1144-1145.
- 22 P. H. Hu, H. J. Kang, J. Chen, J. X. Deng and X. R. Xing, *J. Mater. Chem.*, 2011, **21**, 16205-16209.
- 23 Z. Pan, J. Chen, X. Jiang, Z. S. Lin, L. L. Fan, Y. C. Rong, L. Hu, H. Liu, Y. Ren, X. J. Kuang and X. R. Xing, *Inorg. Chem.*, 2017, **56**, 2589-2595.
- 24 G. Shirane and A. Takeda, *J. Phys. Soc. Jpn.*, 1952, **7**, 1-4.
- 25 P. A. Mante, C. C. Stoumpos, M. G. Kanatzidis and A. Yartsev, *J. Phys. Chem. Lett.*, 2018, **9**, 3161-3166.
- 26 E. C. Subbarao, *J. Am. Ceram. Soc.*, 1960, **4**, 439-442.
- 27 Y. C. Rong, M. L. Li, J. Chen, M. Zhou, K. Lin, L. Hu, W. X. Yuan, W. H. Duan, J. X. Deng and X. R. Xing, *Phys. Chem. Chem. Phys.*, 2016, **18**, 6247-6251.
- 28 X. R. Xing, J. X. Deng, J. Chen and G. R. Liu, *Rare Metals*, 2003, **22**, 294-297.
- 29 R. Yu, H. Hojo, K. Oka, T. Watanuki, A. Machida, K. Shimizu, K. Nakano and M. Azuma, *Chem. Mater.*, 2015, **27**, 2012-2017.
- 30 S. C. Abrahams, S. K. Kurtz and P. B. Jamieson, *Phys. Rev.*, 1968, **172**, 551-553.
- 31 S. J. Clark, M. D. Segall, C. J. Pickard, P. J. Hasnip, M. J. Probert, K. Refson and M. C. Payne, *Z. Krist.-Cryst. Mater.*, 2005, **220**, 567-570.
- 32 W. Kohn and L. J. Sham, *Phys. Rev.*, 1965, **140**, A1133-A1138.
- 33 M. C. Payne, M. P. Teter, D. C. Allan, T. A. Arias and J. D. Joannopoulos, *Rev. Mod. Phys.*, 1992, **64**, 1045-1097.
- 34 J. P. Perdew, K. Burke and M. Ernzerhof, *Phys. Rev. Lett.*, 1996, **77**, 3865-3868.
- 35 J. P. Perdew and Y. Wang, *Phys. Rev. B*, 1992, **46**, 12947-12954.
- 36 D. R. Hamann, M. Schluter and C. Chiang, *Phys. Rev. Lett.*, 1979, **43**, 1494-1497.
- 37 L. Kleinman and D. M. Bylander, *Phys. Rev. Lett.*, 1982, **48**, 1425-1428.
- 38 L. Bellaiche and D. Vanderbilt, *Phys. Rev. B*, 2000, **61**, 7877-7882.
- 39 H. J. Monkhorst and J. D. Pack, *Phys. Rev. B*, 1976, **13**, 5188-5192.
- 40 G. Shirane, R. Pepinsky and B. C. Frazer, *Acta Crystallogr.*, 1956, **9**, 131-140.
- 41 P. W. Stephens, *J. Appl. Crystallogr.*, 1999, **32**, 281-289.
- 42 J. Frantti, S. Ivanov, S. Eriksson, H. Rundlöf, V. Lantto, J. Lappalainen and M. Kähkönen, *Phys. Rev. B*, 2002, **66**, 064108.
- 43 F. F. Wang, Y. Xie, J. Chen, H. G. Fu and X. R. Xing, *Phys. Chem. Chem. Phys.*, 2014, **16**, 5237-5241.
- 44 J. Chen, X. R. Xing, R. B. Yu and G. R. Liu, *Appl. Phys. Lett.*, 2005, **87**, 231915.
- 45 J. Chen, X. R. Xing, G. R. Liu, J. H. Li and Y. T. Liu, *Appl. Phys. Lett.*, 2006, **89**, 101914.
- 46 Z. Pan, J. Chen, R. Z. Yu, L. Patra, P. Ravindran, A. Sanson, R. Milazzo, A. Carnera, L. Hu, L. Wang, H. Yamamoto, Y. Ren, Q. Z. Huang, Y. Sakai, T. Nishikubo, T. Ogata, X. A. Fan, Y. W. Li, G. Q. Li, H. Hojo, M. Azuma and X. R. Xing, *Chem. Mater.*, 2019, **31**, 1296-1303.
- 47 X. G. Zheng, H. Kubozono, H. Yamada, K. Kato, Y. Ishiwata and C. N. Xu, *Nat. Nanotech.*, 2008, **3**, 724-726.
- 48 H. Yamamoto, T. Imai, Y. Sakai and M. Azuma, *Angew. Chem. Int. Ed.*, 2018, **57**, 8170-8173.

Table of Contents



With the introduction of $\text{Bi}(\text{Zn}_{1/2}\text{V}_{1/2})\text{O}_3$, both the tetragonality and negative thermal expansion of PbTiO_3 have been enhanced.